

## Accepted Manuscript

Title: Solar cell with multilayer structure based on nanoparticles composite

Authors: Hala J. El-Khozondar, Rifa J. El-Khozondar, Mohammed M. Shabat, Daniel M. Schaadt



PII: S0030-4026(18)30495-9  
DOI: <https://doi.org/10.1016/j.ijleo.2018.04.014>  
Reference: IJLEO 60742

To appear in:

Received date: 3-3-2018  
Accepted date: 3-4-2018

Please cite this article as: El-Khozondar HJ, El-Khozondar RJ, Shabat MM, Schaadt DM, Solar cell with multilayer structure based on nanoparticles composite, *Optik* (2018), <https://doi.org/10.1016/j.ijleo.2018.04.014>

This is a PDF file of an unedited manuscript that has been accepted for publication. As a service to our customers we are providing this early version of the manuscript. The manuscript will undergo copyediting, typesetting, and review of the resulting proof before it is published in its final form. Please note that during the production process errors may be discovered which could affect the content, and all legal disclaimers that apply to the journal pertain.

# Solar cell with multilayer structure based on nanoparticles composite

Hala J. El-Khozondar<sup>a,\*</sup>, Rifa J. El-Khozondar<sup>b</sup>, Mohammed M. Shabat<sup>c</sup>, Daniel M. Schadt<sup>d</sup>

<sup>a</sup>Electrical Engineering Department, Islamic University of Gaza, Gaza, Palestine

<sup>b</sup>Physics Department, Al-Aqsa University, Gaza, Palestine

<sup>c</sup>Physics Department, Islamic University of Gaza, Gaza, Palestine

<sup>d</sup>Institute of Energy Research and Physical Technologies, Clausthal University of Technology, Leibnizstr. 4, 38678 Clausthal-Zellerfeld, Germany

**ABSTRACT-** In this study, a four-layer waveguide structure has been investigated as a solar cell model. In the proposed structure, a nanoparticle composite layer is added to enhance the efficiency of the solar cell due to their ability of controlling the light transmission and reflection. The nanoparticles are taken to be a mixture of Ag and Au embedded in a dielectric media consists of polyacrylic acid laid above a SiN<sub>x</sub> antireflection coating layer. Both layers are sandwiched between glass substrate and air cladding. The average reflectance for TE and TM fields are calculated using Maple. Results show that the reflectance depends on the ratio of the nanoparticle in the dielectric media, refractive index of SiN<sub>x</sub> layer and the angle of incidence. Thus, the performance of solar cell has been optimized by tuning and adjusting the above-mentioned parameters.

**Keywords:** Nanoparticles, Antireflection coating, Reflectance, Solar energy, Solar cell.

## 1. Introduction

Solar cells are widely used as a building block for solar systems. Solar cells, which is also known as photovoltaic (PV) cells, convert absorbed sun light to electrical energy. Recently, solar cell models based on nanoparticles have been extensively investigated in order to enhance solar cell efficiencies [1-3]. Particularly, they may be used to obtain zero reflection due to their ability to absorb light if they used at a specified ratio. Materials such as SiN<sub>x</sub> are used like antireflection coating layer for high refractive index, which can be easily varied by varying the deposition parameters [4-7]. For this reason, they are used intensively to improve the efficiency of solar cells as single or double antireflection coating layer [4,7,8].

Oh et al. [5] investigated the features that affect potential-induced degradation of the shunting type. Among these features are the parts of refractive index of SiN<sub>x</sub> antireflection coating in addition to emitter sheet resistance. Hsu et al. [6] were able to apply the hydrogenated amorphous silicon nitride (a-SiN<sub>x</sub>:H) as a refractive index (n) equivalent deposits in the middle of glass (n=1.5) and the transparent conducting oxide (n=2). It is shown that the solar cell performance is enhanced by changing the refractive index and thickness of the a-SiN<sub>x</sub>:H deposits.

El-Amassi et al. [2] reported that PV cell efficiency could be improved by using metamaterial

---

\* Corresponding author.

E-mail address: hkhonzondar@iugaza.edu (H. El-Khozondar).

(MTM) and SiNx layers surrounded by glass and by air. El-Khozondar et al. [1] considered dissipative MTM for the same structure to measure the effect of dissipation. In other work, nanoparticles embedded in a dielectric media is used to further control the efficiency of the solar cell [3].

In this study, we employed a composite nanoparticle made of Ag-Au embedded in a dielectric media between SiNx layer from bottom and air from top. In the following section, the theory will be developed. Section 3 is dedicated to exhibit the results and discussions followed by conclusion.

## 2. Theory

The simple schematic proposed structure is a four-layer solar cell as shown in Fig. 1. The SiNx antireflection coating layer is placed on a glass substrate. The nanoparticle-composite sheet is sandwiched between SiNx antireflection coating layer from below and air layer from above. The nanoparticle-composite layer is taken to be Ag-Au embedded in polyacrylic acid host media with thickness  $d_1$  and effective refractive index  $n_1$ . SiNx layer has a thickness  $d_2$  and refractive index  $n_2$ . Glass layer has refractive index  $n_s$  and air has refractive index  $n_0$ .

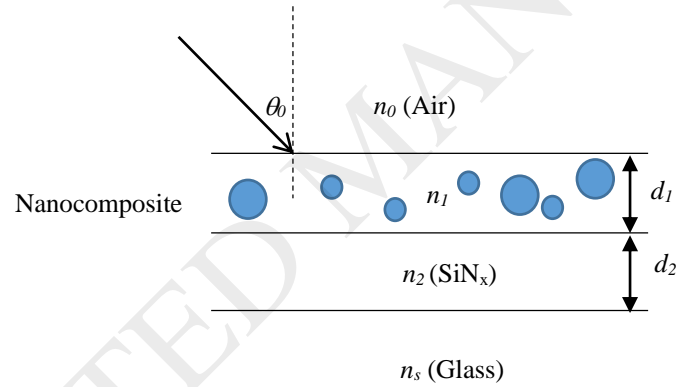


Fig. 1. Proposed solar cell structure

The effective permittivity for the nanocomposite layer ( $\epsilon_l$ ) is calculated using Dynamical Maxwell-Garnett theory (Eq. 1) which is an extended version of Maxwell-Garnett theory [9]. The theory assumes that the host (in our case is polyacrylic acid) is the majority and the metal nanoparticles (Au and Ag) are the annexation materials with chosen metal fraction in the composite [9-11].

$$\frac{\epsilon_l - \epsilon_h}{\epsilon_l + 2\epsilon_h} = f_{Ag} \frac{\epsilon_{Ag} - \epsilon_h}{\epsilon_{Ag} + 2\epsilon_h + (\epsilon_h - \epsilon_{Ag})(1 - f_{Ag})\alpha} + f_{Au} \frac{\epsilon_{Au} - \epsilon_h}{\epsilon_{Au} + 2\epsilon_h + (\epsilon_h - \epsilon_{Au})(1 - f_{Au})\alpha} \quad (1)$$

where  $\epsilon_{Ag}$  is the permittivity of silver nanometal,  $\epsilon_{Au}$  is the permittivity of gold nanometal,  $\epsilon_h$  is the permittivity of polyacrylic acid,  $f_{Ag}$  and  $f_{Au}$  are the silver nanoparticle and gold nanoparticle volume fractions. The particle size effect is introduced via  $\alpha$  [9,10] as follows

$$\alpha = x^2 + i \left( \frac{2}{3} \right) x^3 \quad (2)$$

where  $x = \varepsilon_h \sqrt{(\omega a)/c}$ ,  $\omega$  is the angular frequency,  $a$  is the radius of the metal nanoparticle, and  $c$  is the speed of light. The value of  $a$  is assumed to be an average value which equals to 20 nm. Once  $\varepsilon_l$  is calculated, the value of effective refractive index  $n_l$  is obtained by taking square root of  $\varepsilon_l$ .

To understand the performance of the proposed structure, the light assumed to strike the solar cell air-nanocomposite interface at oblique incidence with an incidence angle ( $\theta_0$ ) that can adopt different values. For oblique incidence, the optical admittance for the  $k_{th}$  layer is derived in the paper of [12,13] for both transverse electric field polarization (TE) and transvers magnetic field polarization (TM) as follows

$$\gamma_k^{TE} = \frac{1}{\eta_0 \mu_k} n_k \cos \theta_k \quad (3)$$

$$\gamma_k^{TM} = \frac{1}{\eta_0 \mu_k} \frac{n_k}{\cos \theta_k} \quad (4)$$

where  $\eta_0 = \sqrt{\mu_0 / \varepsilon_0}$  is the air intrinsic impedance. The angle  $\theta_k$  is related to  $\theta_0$  by Snell's law:

$$n_0 \sin \theta_0 = n_k \sin \theta_k; \quad k = 1, 2, \dots, m \quad (5)$$

The 2x2 transfer matrix that relates the field components at two successive boundaries (e.g. 1 and 2) is defined as [1,2,14,15]

$$M_k = \begin{bmatrix} m_{11} & m_{12} \\ m_{21} & m_{22} \end{bmatrix} = \begin{bmatrix} \cos(\delta_k) & \frac{i \sin(\delta_k)}{\gamma_k} \\ i \gamma_k \sin(\delta_k) & \cos(\delta_k) \end{bmatrix} \quad (6)$$

where  $\delta_k = 2\pi n_k d_k \cos(\theta_k)/\lambda$  is the phase difference.

Assume that  $E_2$  and  $B_2$  are the electric field and the magnetic field density at boundary “2” and  $E_1$  and  $B_1$  are the electric field and the magnetic field density at boundary “1”, then they are related as follows:

$$\begin{bmatrix} E_1 \\ B_1 \end{bmatrix} = M_k \begin{bmatrix} E_2 \\ B_2 \end{bmatrix} \quad (7)$$

For  $m$  layers, the overall transfer matrix ( $M_T$ ) is defined in terms of individual matrix as

$$M_T = M_1 M_2 \dots M_m = \prod_{k=1}^m M_k \quad (8)$$

Then, the reflectance can be derived from Eq. (5) and Eq. (6). The reflectance  $R = |r|^2$  where  $r$  is the reflection coefficient defined as [16,10]

$$r = \frac{E_{r1}}{E_0} = \frac{m_2}{m_1} \quad (9)$$

Following the reflectance  $R^{TE}$  and  $R^{TM}$  for both TE and TM polarization are derived for the proposed structure [12, 13]. The total reflectance  $R$  for the solar cell is taken to be the average value of  $R^{TE}$  and  $R^{TM}$  as in Eq. (10).

$$R = \frac{R^{TE} + R^{TM}}{2} \quad (10)$$

### 3. Results and Discussion

To obtain the total average reflectance  $R$ , Equation 10, has been solved numerically using Software Maple 17. In our calculations, we choose the operating wavelength to vary from 400 nm to 1200 nm following previous work [1,3,17-21]. The values of  $d_1$  and  $d_2$  are selected to be equal quarter wavelength in the media. The values of dielectric permittivity for Ag and Au nanoparticles are respectively [22]:  $\epsilon_{Ag} = -15.493 + j0.36873$  and  $\epsilon_{Au} = -9.5160 + j1.3133$ . The value of refractive index for polyacrylic acid is 1.5270 [9]. The refractive index for SiNx ( $n_2$ ) may assume different values between 1.78 and 2.3 [4-7]. The refractive index for air and substrate are  $n_0 = 1$  and  $n_s = 1.47$  respectively.

Initially, the average reflectance  $R$  versus the operating wavelength for normal incidence has been computed as shown in Fig. 2-Fig. 5. Then, we perform the same calculation for oblique incidence (see Fig. 6). Fig. 2 displays the dependence of  $R$  on the wavelength at  $f_{Ag}:f_{Au} = 1:3.4$  for different values of  $n_2$  where the solid curve, dash curve, dotted curve and dash-dot curve correspond to  $n_2 = 2.1, 2, 1.9, 1.8$  respectively. For all the curves, the value of  $R$  decreases as  $\lambda$  increases until it reaches a minimum value around  $\lambda = 640\text{nm}$ , then, it increases again. It is also clear that as  $n_2$  decreases the value of  $R$  decreases to reach its minimum at  $n_2 = 1.8$ . This can be explained from Eq. (9) where  $R$  is directly

proportional to the square of  $m_{2l}$  which directly proportionality to the refractive index.

To find the effect of the volume fraction between Ag and Au on  $R$ , we repeat the previous calculation for  $f_{Ag}:f_{Au}=1:6$  and  $1:1.8$  in Fig. 3 and Fig. 4 respectively. Comparing Fig. 2, 3, and 4, we can easily realize that as the fraction of Au gets smaller, the reflection decreases to reach its minimum at  $f_{Ag}:f_{Au}=1:1.8$ . This is clearly presented in Fig. 5 where the value of  $R$  is plotted versus the wavelength at  $n_2=1.8$  (where the values of  $R$  have the minima) for the three values of  $f_{Ag}:f_{Au}$ . Fig. 5 illustrates that as the fraction of Au gets smaller, the value of  $\lambda$ , at which the minimum of  $R$  occurs, has blue shift. This is because the Ag has higher absorption coefficient.

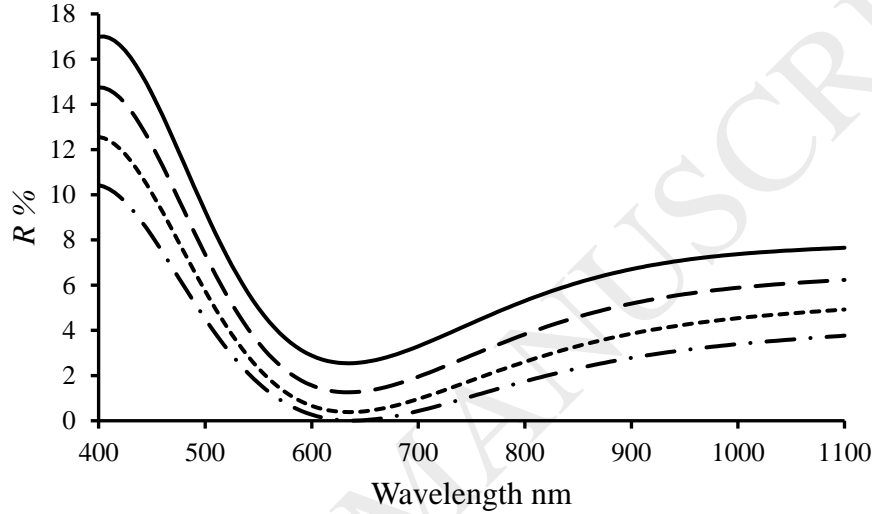


Fig. 2. The reflectance versus the operating wavelength,  $\lambda$  nm at different values of  $n_2$  for Ag to Au volume fraction=1:3.4. Solid curve corresponds to  $n_2=2.1$ , dash curve corresponds to  $n_2=2$ , dotted curve corresponds to  $n_2=1.9$ , dash-dot curve corresponds to  $n_2=1.8$ .

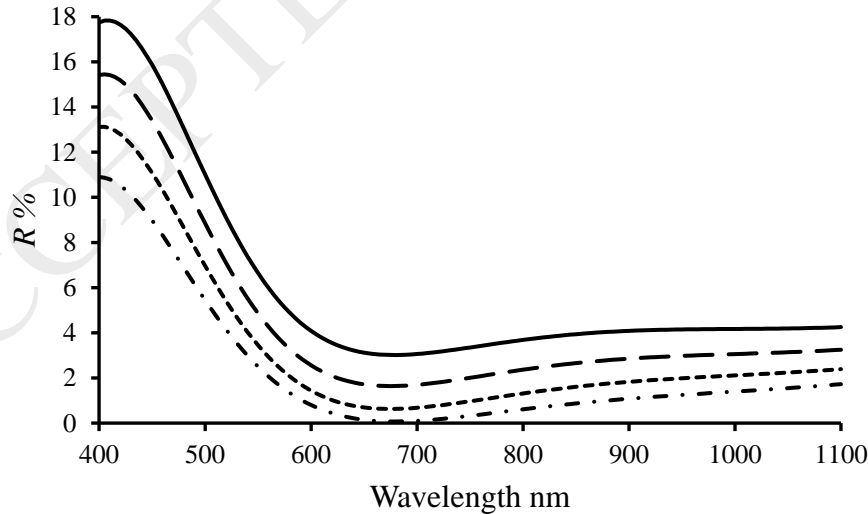


Fig. 3. The reflectance versus the operating wavelength,  $\lambda$  nm at different values of  $n_2$  for Ag to Au volume fraction=1:6. Solid curve corresponds to  $n_2=2.1$ , dash curve corresponds to  $n_2=2$ , dotted curve corresponds to  $n_2=1.9$ , dash-dot curve corresponds to  $n_2=1.8$ .

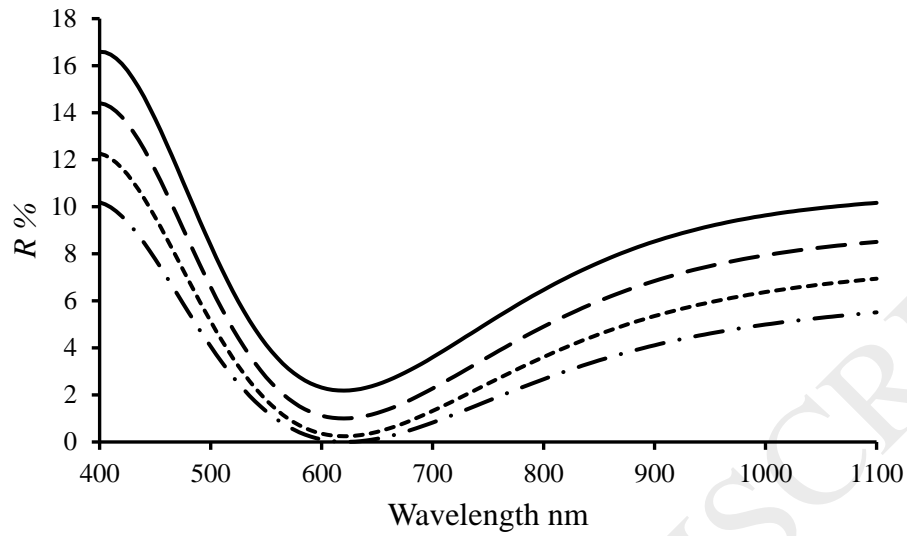


Fig. 4. The reflectance versus the operating wavelength,  $\lambda$  nm at different values of  $n_2$  for Ag to Au volume fraction=1:1.8. Solid curve corresponds to  $n_2=2.1$ , dash curve corresponds to  $n_2=2$ , dotted curve corresponds to  $n_2=1.9$ , dash-dot curve corresponds to  $n_2=1.8$ .

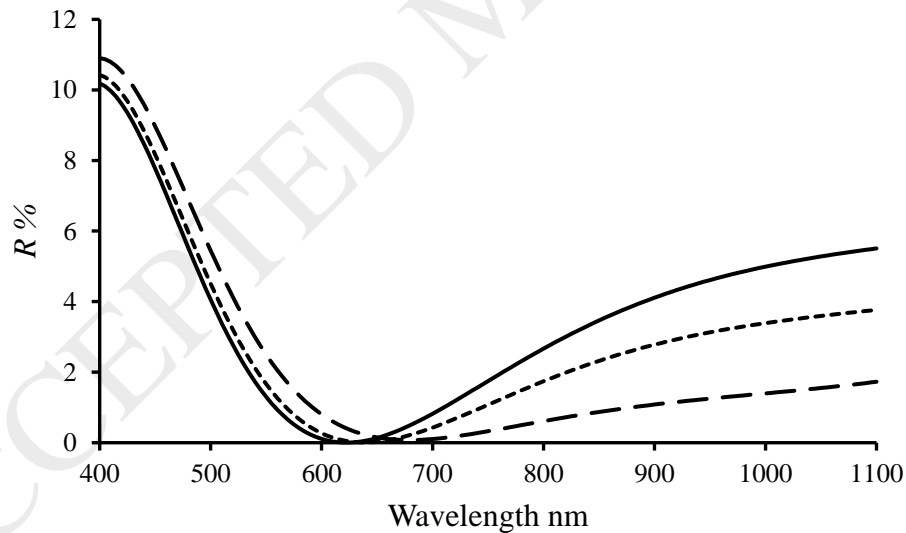


Fig. 5. The reflectance versus the operating wavelength,  $\lambda$  nm at  $n_2 = 1.8$  and for Ag to Au volume fraction equals 1:1.8 (Solid curve), 1: 6 (dash curve) and 1:3.4 (dotted curve).

For oblique incidence, the calculations are repeated for  $\theta = 15^\circ, 30^\circ, 45^\circ, 60^\circ$ . The calculations are performed at  $n_2 = 1.8$  and  $f_{\text{Ag}}:f_{\text{Au}} = 1:1.8$  where  $R$  has its minimum. Fig. 6 displays  $R$  as a function of wavelength for  $\theta = 60^\circ, 45^\circ, 30^\circ, 15^\circ, 0^\circ$  indicated by solid line, dash line, dash-dot line, dotted line, and dash-double dot line respectively. Normal incidence  $0^\circ$  is added for comparison.

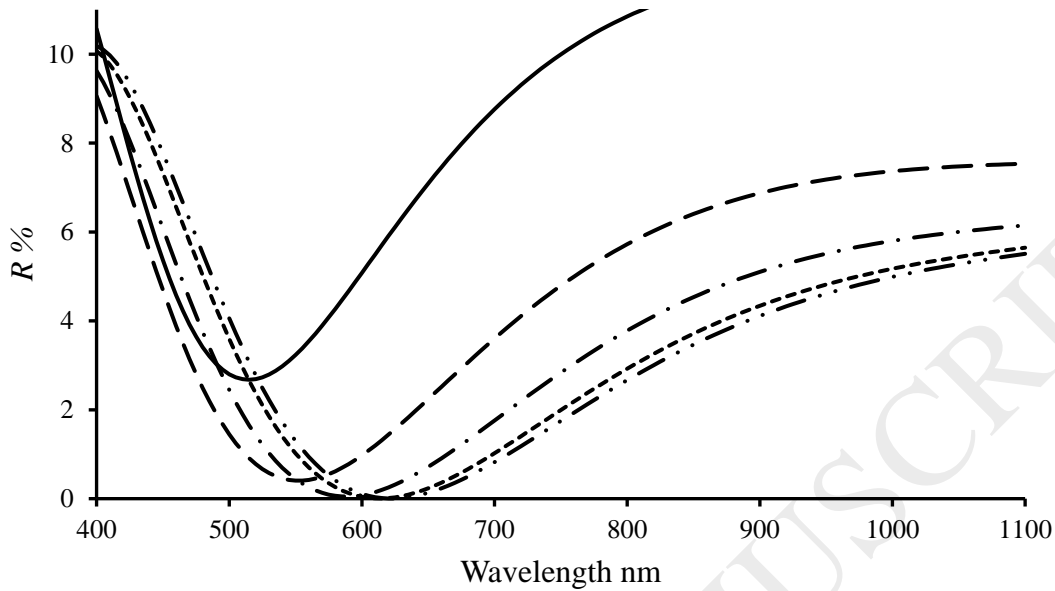


Fig. 6. The reflectance for oblique incidence versus  $\lambda$  at  $n_2 = 1.8$  and Ag to Au volume fraction equals 1:1.8. Solid line is for  $\theta_0 = 60^\circ$ , dash line is for  $\theta_0 = 45^\circ$ , dash-dot line is for  $\theta_0 = 30^\circ$ , dotted line is for  $\theta_0 = 15^\circ$ , and dash-double dot line corresponds to  $\theta_0 = 0^\circ$ .

From Fig. 6, we can conclude that the reflectance is highly dependent on the angle of incidence and the value of  $\lambda$  at which minimum occurs also changes. In addition, it has been observed that the change is big for  $\theta_0 = 60^\circ$ . Moreover, there is a red shift as  $\theta_0$  decreases. All the computed figures have clearly shown that the minimum reflectance can effectively be obtained by controlling the light incident angles and contents of the nanoparticle layer.

#### 4. Conclusion

A Multilayer antireflection coating have been modeled in which a nano-composite layer is added on top of SiNx ARC layer. The nanometals used in the work are Ag and Au. The effect of the refractive index of SiNx layer and the volume fraction of Ag to Au nanoparticles on the reflectance has been studied for both normal and oblique incidence. It is found that we may control the minimum of the reflectance as well as the value of wavelength at which minimum might occur by varying the refractive index of SiNx layer or/and by changing the ratio of Ag to Au. Moreover, it is noticed that the smaller the incidence angle, the smaller the value of reflectance. The obtained promising results could be used in design and manufacture future solar cells.

## References

- [1] H.J. El-Khozondar, D.M. El-Amassi, M. M. Shabat, Modification of PV behavior using dissipative MTM, in Proceedings of META16 conference, Malaga, Spain, 2016, pp. 1564-1567.
- [2] D.M. El-Amassi, H.J. El-Khozondar, M.M. Shabat, Efficiency enhancement of solar cell using metamaterials, *Int. J. Nano Stud. Technol.* 4 (2015) 84–87.
- [3] M.M. Shabat, D.M. El-Amassi, D.M. Schaadt, Design and analysis of multilayer waveguides with different substrate media and nanoparticles for solar cells, *Solar Energy Journal* 137 (2016) 409–412.
- [4] D. Gong, Y.J. Lee, M. Ju, J. Ko, D. Yang, Y. Lee, G. Choi, S. Kim, J. Yoo, B. Choi and J. Yi, SiNx double layer antireflection coating by plasma-enhanced chemical vapor deposition for single crystalline silicon solar cells, *Jpn. J. Appl. Phys.* 50 (2011) 08KE01-5.
- [5] J. Oh, B. Dauksher, S. Bowden, G. Tamizhmani, P. Hacke, J. D'Amico, Further Studies on the Effect of SiNx Refractive Index and Emitter Sheet Resistance on Potential-Induced Degradation, *IEEE Journal of Photovoltaics* 7 (2017) 437-443.
- [6] C.H. Hsu, Y.P. Lin, H.J. Hsu, C.C. Tsai, Enhanced spectral response by silicon nitride index matching layer in amorphous silicon thin-film solar cells, *Journal of Non-Crystalline Solids* 358 (2012) 2324-2326.
- [7] Y. Lee, D. Gong, N. Balaji, Y. Lee, J. Yi, Stability of SiNX/SiNX double stack antireflection coating for single crystalline silicon solar cells, *Nanoscale Res. Lett.* 7 (2012) 50-55.
- [8] M. Beye, M.E. Faye, A. Ndiaye, F. Ndiaye, A.S. Maiga, Optimization of SiNx Single and Double Layer ARC for Silicon Thin Film Solar Cells on Glass. *Research Journal of Applied Sciences, Engineering and Technology* 6 (2013) 412-416.
- [9] R. Kitsomoboona, C. Ngambenjawan, W.S. Mohammed, M.B. Chaudhari, G.L. Hornyak, J. Dutta, Plasmon resonance tuning of gold and silver nanoparticle-insulator multilayered composite structure for optical filters, *Micro & Nano letter* 6 (2011) 342-344.
- [10] R. Rupp, Evaluation of extended Maxwell-Garnett theories, *Opt. Commun.* 182 (2000) 273–279.
- [11] Z. Shi, G. Piredda, A.C. Liapis, M.A. Nelson, L. Novotny, R.W. Boyd, Surface-Plasmon polaritons on metal-dielectric nanocomposite films, *Opt. Lett.* 34 (2009) 3535-3537.
- [12] S. Al-Turk, Analytic optimization modeling of anti-reflection coating for solar cells, Master thesis, MacMaster University, 2011.
- [13] M. Lequime, B. Gralak, S. Guenneau, M. Zerrad, C. Amra, Optical properties of multilayer optics including negative index materials, *Physics.Optics*, arXiv:1312.6288v1 (2013) 1-9.
- [14] C.C. Katsidis, D.I. Siapkas, General transfer-matrix method for optical multilayer systems with coherent, partially coherent, and incoherent interference, *Applied Optics* 41 (2002) 3978–3987.
- [15] M.C. Tropicovsky, A.S. Sabau, A.R. Lupini, Z. Zhang, Transfer-matrix formalism for the calculation of optical response in multilayer systems: from coherent to incoherent interference, *Optics Express* 18 (2010) 24715–24721.
- [16] D.M. Schaadt, B. Feng, E.T. Yu, Enhanced semiconductor optical absorption via surface plasmon excitation in metal nanoparticles, *Appl. Phys. Lett.* 86 (2005) 063106.
- [17] G.E. Jonsson, H. Fredriksson, R. Sellappan, D. Chakarov, Nanostructures for enhanced light

- absorption in solar energy devices, *Int. J. Photoenergy* (2011) 1–11.
- [18] S. Saylan, T. Milakovich, S.A. Hadi, A. Nayfeh, E.A. Fitzgerald, M.S. Dahlem, Multilayer antireflection coating design for GaAs<sub>0.69</sub>P<sub>0.31</sub>/Si dual-junction solar cells, *Sol. Energy* 122 (2015) 76–86.
- [19] S. Pillai, M.A. Green, Plasmonics for photovoltaic applications. *Sol. Energy Mater, Sol. Cells* 94 (2010) 1481–1486.
- [20] Y. Huihui, J. Rui, C. Chen, D. Wuchang, W. Deqi, L. Xinyu, Antireflection properties and solar cell application of silicon nanostructures, *J. Semiconduct.* 32 (2011) 0840051-6.
- [21] C.R. Simovski, A.S. Shalin, P.M. Voroshilov, P.A. Belov, Photovoltaic absorption enhancement in thin-film solar cells by nonresonant beam collimation by submicron dielectric particles, *J. App. Phys.* 114 (2013) 103104.
- [22] K.M. McPeak, S.V. Jayanti, S.J.P. Kress, S. Meyer, S. Iotti, A. Rossinelli, and D. J. Norris, Plasmonic films can easily be better: Rules and recipes, *ACS Photonics* 2 (2015) 326-333.